NON-LINEAR EFFECTS AT RANGE FROM UNDERWATER EXPLOSIONS

H. W. Marsh
Naval Underwater Systems Center

INTRODUCTION

Recordings of pressure waveforms from underwater explosives have been previously reported.[1] Further results and theoretical calculations are reported elsewhere in detail.[2] In addition, measurements and theory involving radiation from a directional CW source have been reported.[3] The present writing will be confined to comments on the theory and its agreement with experiment.

The hydrodynamical field equations simplify in the unidimensional case, where the pressure (say) is a function only of time and a single space variable, and where there is but one ray connecting a pair of points in the three-dimensional space. Examples would be plane cylindrical or spherical waves, or refracted rays in an unbounded medium with monotonic velocity gradient. For small nonlinearity, in a viscous, thermally radiating medium, the normalized pressure y in the farfield of a source is thus describable by the equation

$$(q + \partial/\partial\tau)y_x = (q + \partial/\partial\tau)(yy_\tau) + f(x)(q\xi_1 y_{\tau\tau} + \xi_2 y_{\tau\tau\tau}) . \qquad (1)$$

In Eq. (1), x is the space coordinate ($f(x)$ accounts for geometrical spreading) and τ the local time, which would be $t - x/c$ for a constant velocity c; q is the radiation coefficient and may be formally identified as the relaxation frequency of a simple relaxation process; and ξ_1 and ξ_2 are the dissipation coefficients for relaxation and viscosity, respectively. The whole we call "Generalized Burger's Equation"; all quantities are consistently dimensionalized.

If the waveform $p(\tau, x_o)$ is known from some point x_o, Eq. (1) can be integrated to provide the waveform at other points x. We have performed such integrations using finite differences with time increment T and space increment X. Special care must be taken near the beginning and end of waveforms of finite duration.

RESULTS—EXPLOSIVES

Four-lb sofar charges were detonated at a depth of 1200 meters, and waveforms recorded at slant ranges between 1500 and 20,000 meters. The first positive phase (later phases will not be discussed) consists of a leading edge with rise time of several μsec, a peak and linear decay for some 400 μsec. Given the waveform at 1500 meters, waveforms at other ranges can be computed from Eq. (1). Assuming spherical spreading at range r, we have $x = \log(r/r_o)$, $f(x) = \exp(x)$, and y is the pressure compensated for the assumed spreading. For discrete time and space values we use $\tau = nT$, $x = mX$, with $T = 1\,\mu$sec and $X = 0.0028$. With this value of X, the relationship between the integer m and range is shown in Fig. 1.

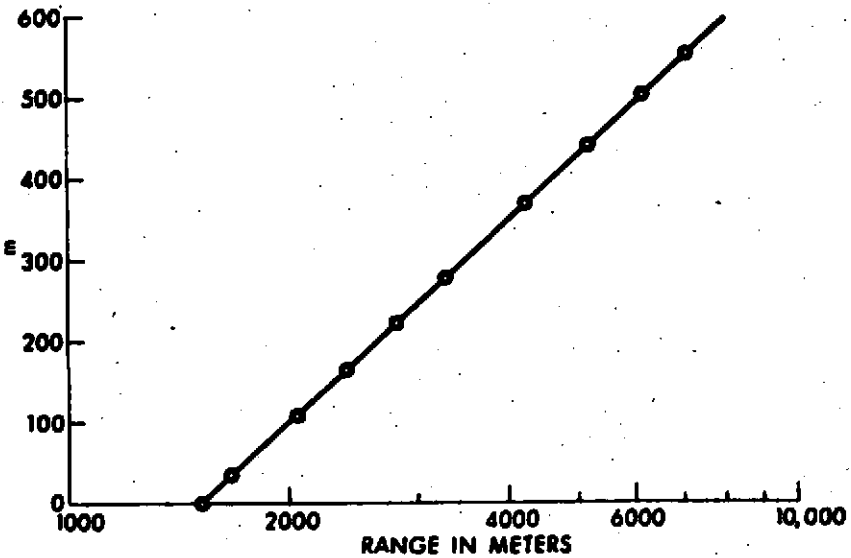

Fig. 1. Relation of Parameter m to Range. Circles Denote Ranges Corresponding to Shot Records.

A sequence of waveform leading edges is shown in Fig. 2. The highest, at the right is that recorded at 1500 meters; the balance are computed. Figure 3 shows the comparison between a calculation at about 4700 meters (m = 400) and recordings at nearby ranges. That finite amplitude is important may be judged from Fig. 4, computed for identical conditions excepting for the neglect of the nonlinear term of Eq. (1). This is accomplished by inserting a numerical factor called "AL," which can have the values 1 or 0.

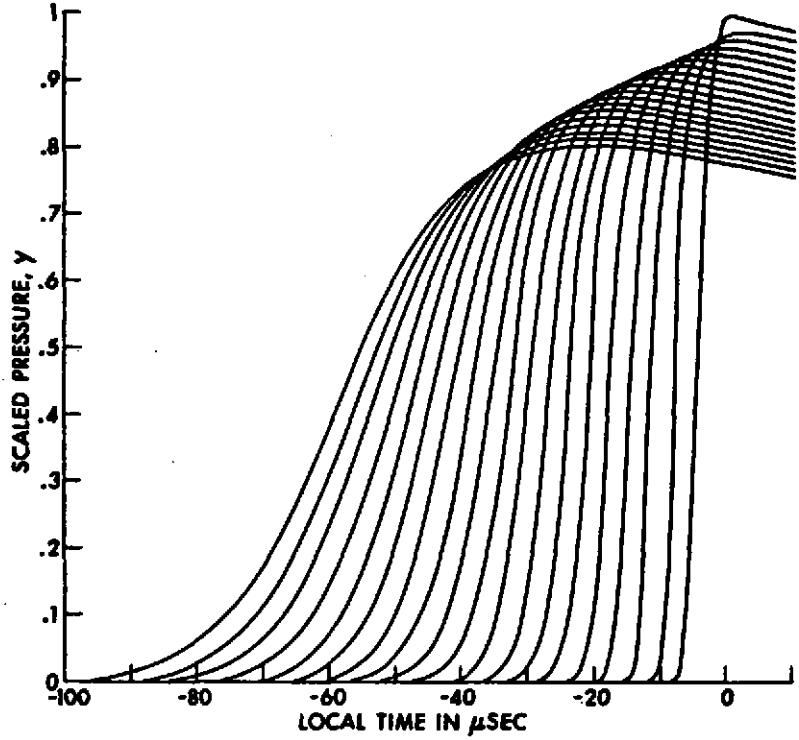

Fig. 2. Computed Waveforms, Run 4 (AL = 1). Curves Are Given for Every Multiple of m = 50 from 0 to 900.

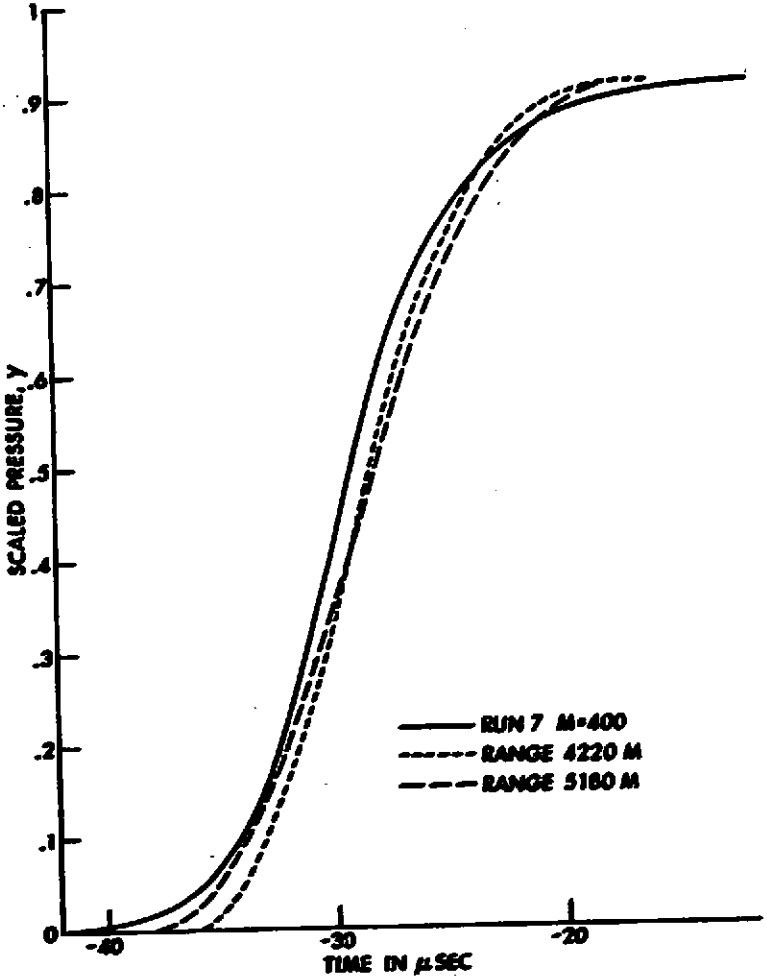

Fig. 2. Comparison of Measured and Computed Waveforms

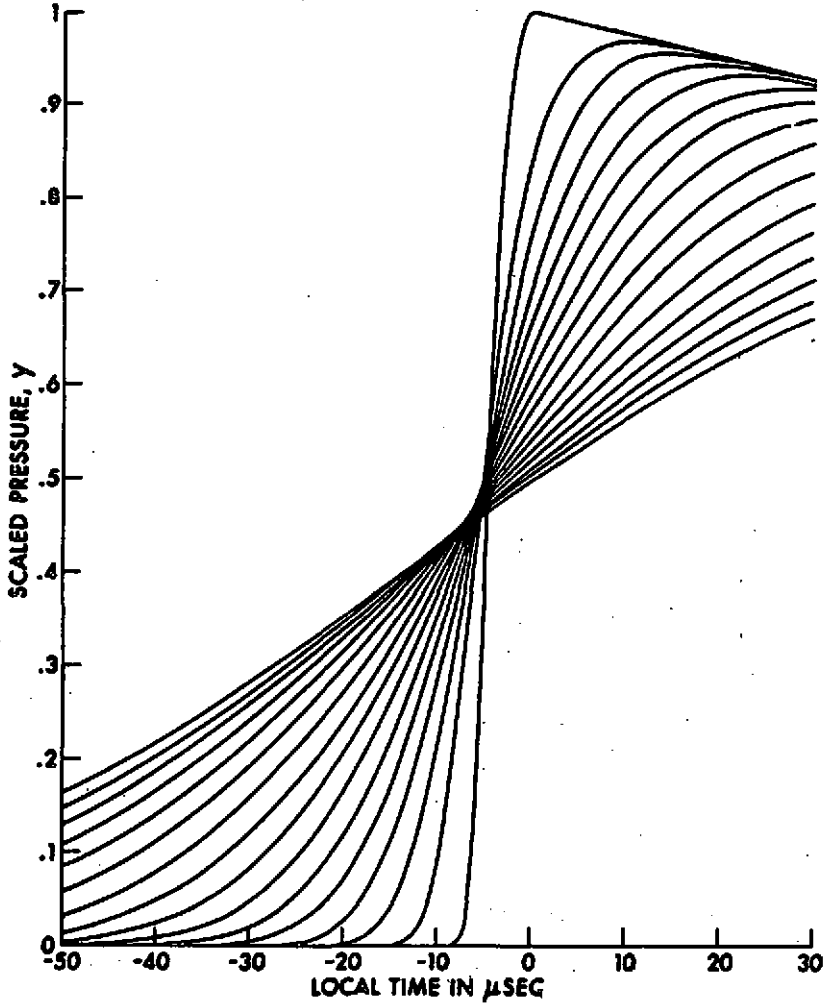

Fig. 4. Computed Waveforms, Run 3 (AL = 0). Curves Are Given for Every Multiple of m = 100 from 0 to 1500.

Figures 5, 6, and 7 show other comparisons between computations and measurements. In Fig. 5 the computations are made with and without nonlinearity; the empirical law of Arons[4] is also shown. In Fig. 6 the rise time is defined to be the reciprocal of the maximum derivate divided by the amplitude at that point: (Y') max/y. The spectra of Fig. 7 are computed for the entire first positive phase. The implied attenuation coefficients are substantially less than would be computed for linear propagation, due to the continued transfer of energy up from the low frequencies where the bulk of the energy resides. There is a corresponding excess attenuation at lower frequencies.

A more complete account of the above results may be found in Reference 2. The generalized Burger's equation appears to account satisfactorily for the propagation of explosive waves, but it does not, in itself, predict the source characteristics of the explosion, or the influence of depth thereupon (e.g., see Christian and Blaik[5]).

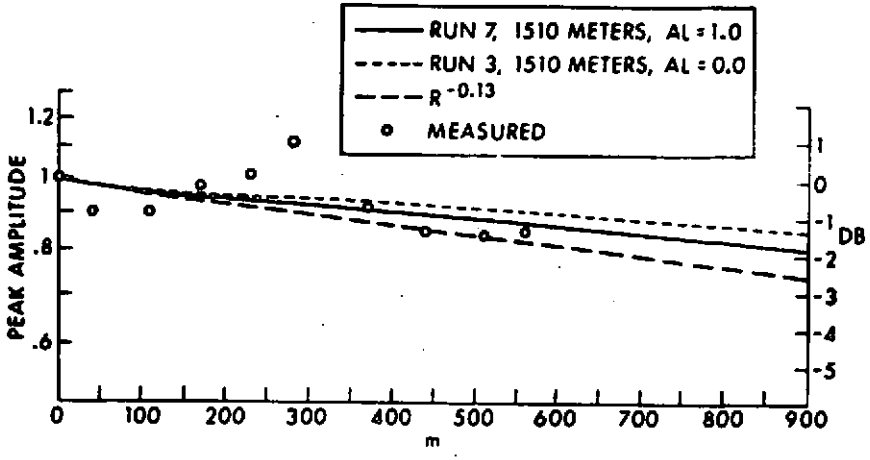

Fig. 5. Comparison of Measured and Computed Peak Pressures

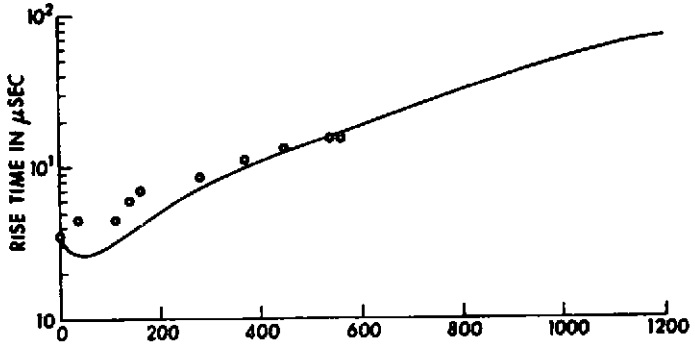

Fig. 6. Comparison of Measured and Computed Rise Times

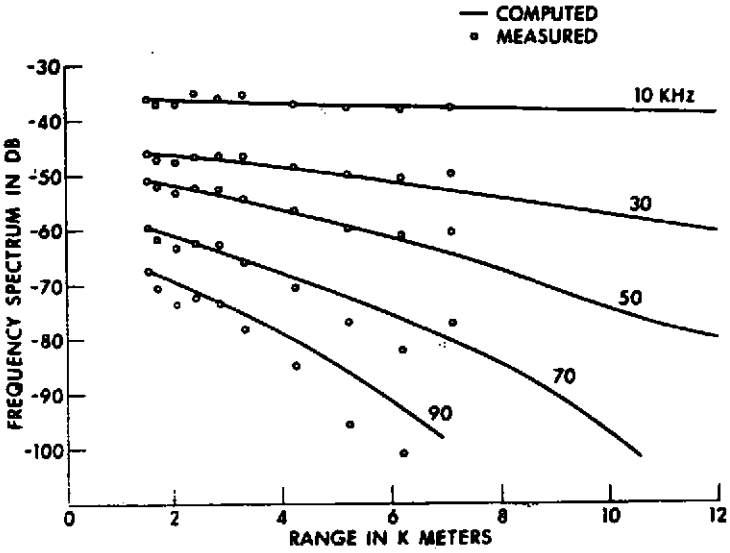

Fig. 7. Comparison of Measured and Computed Spectra. Curves and Data Are Shifted Down 5 and 10 dB at 70 and 90 kHz, Respectively.

RESULTS—DIRECTIONAL CW

CW pulses were transmitted and recorded in the farfield of a directional source. The transmitted pulses were intended to be sinusoidal, but analysis indicates the presence of small, but important, harmonic distortion. The fundamental and harmonics were measured as a function of distance along the maximum response axis of the source. The source is assumed to radiate plane waves for a distance r_o, after which spherical spreading occurs. By use of Eq. (1), the harmonic content can be computed for given initial conditions. Initial conditions were assumed which gave the best fit of the computed curves with the measurements, as follows:

plane wave extent (r_o)	20 meters
second-harmonic content	-30 dB
third-harmonic content	-60 dB

The computations and measurements are shown in Fig. 8. The harmonic content is relative to the fundamental at the range of interest. Parameters

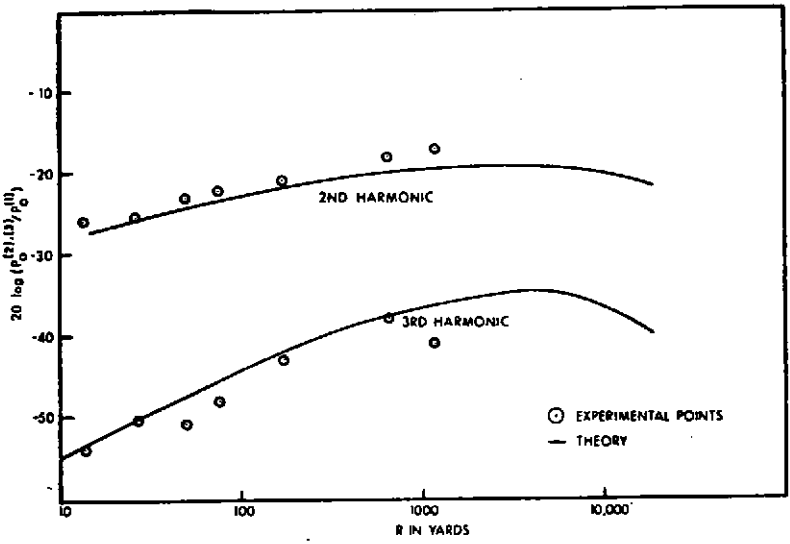

Fig. 8. Calculations Extrapolated to Long-Range Ocean Environment

appropriate to sea water were used in the calculations. The initial harmonic content is especially important for the development of the third harmonic, in effect transforming a third-order effect into a second-order effect. Beam patterns of the fundamental and harmonics are shown in Figs. 9, 10, and 11, where the development of the pattern with range is evident. The 176-yd third-harmonic pattern is nearly the same as that of the corresponding second harmonic, indicating a second-order process. The 650-yd third-harmonic pattern is probably contaminated by direct radiation from the source. The second-order beam patterns are in agreement with the theory of Ingenito.[6] According to our numerical integration of his equations, the second-order beam pattern, in the farfield, is the square of the fundamental beam pattern, independent of frequency.

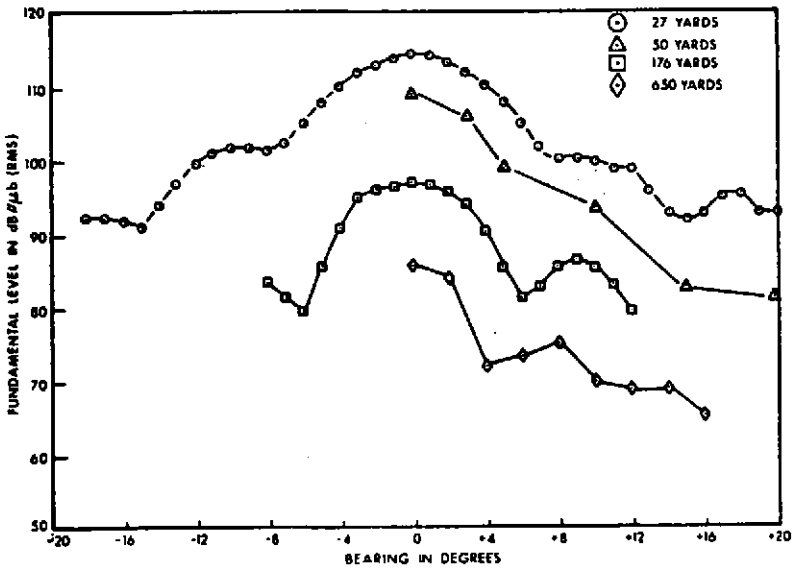

Fig. 9. Fundamental Received Level vs Bearing

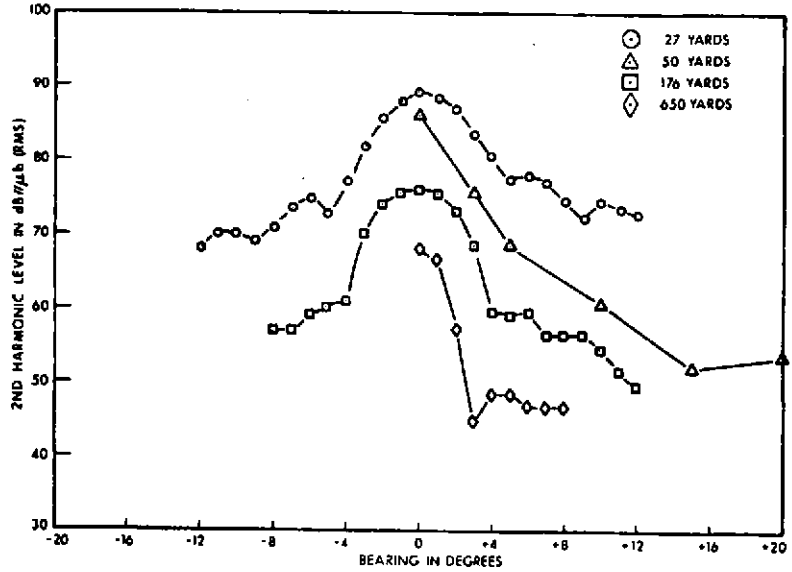

Fig. 10. Second-Harmonic Received Level vs Bearing

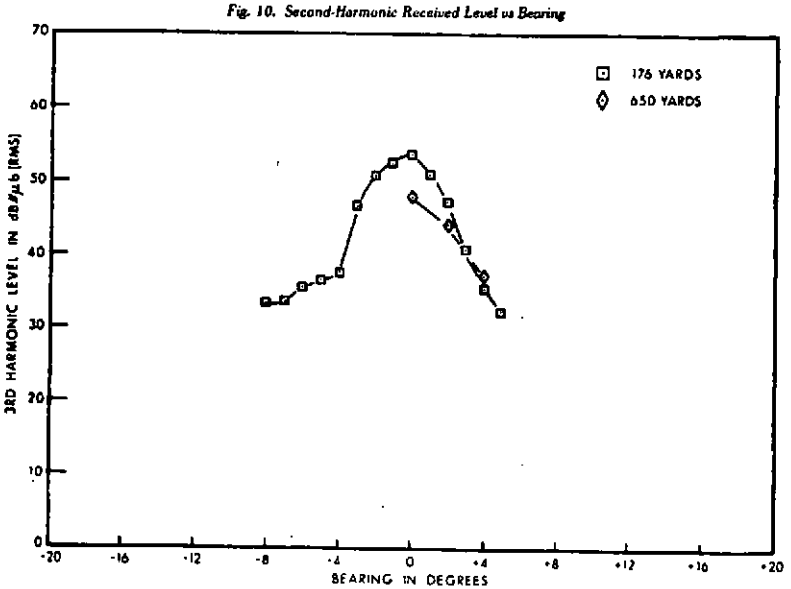

Fig. 11. Third-Harmonic Received Level vs Bearing

REFERENCES

1. H. W. Marsh, R. H. Mellen, and W. L. Konrad, "Anomalous Absorption of Pressure Waves from Explosions in Sea Water," J. Acoust. Soc. Amer., 38, 326-338 (1965).

2. "Propagation and Reception of Transient Underwater Sounds," prepared by AVCO Corp. for ONR Code 468, Contract Nonr 3353(00) (15 Sept 1966).

3. "Underwater Sound Propagation and Reverberation," prepared by AVCO Corp. for NAVSHIPSYSCOM, Contract Nobsr 95176 (1 Oct 1966).

4. A. B. Arons, "Underwater Explosive Shock Wave Parameters at Large Distances from the Charge," J. Acoust. Soc. Amer., 26, 343-346 (1954).

5. E. A. Christian and M. Blaik, "Near-Surface Measurements of Deep Explosions," J. Acoust. Soc. Amer., 38, 50-56 (Part I); 57-62 (Part II) (1965).

6. F. Ingenito, PhD dissertation, Brown University, Physics Dept. (1968).